

ARTICLE

Received 18 Mar 2014 | Accepted 9 Sep 2014 | Published 28 Oct 2014

DOI: 10.1038/ncomms6217

RNAi-based functional selection identifies novel cell migration determinants dependent on PI3K and AKT pathways

Minchul Seo^{1,2,*}, Shinrye Lee^{1,3,*}, Jong-Heon Kim¹, Won-Ha Lee⁴, Guang Hu⁵, Stephen J. Elledge⁶
& Kyoungso Suk¹

Lentiviral short hairpin RNA (shRNA)-mediated genetic screening is a powerful tool for identifying loss-of-function phenotype in mammalian cells. Here, we report the identification of 91 cell migration-regulating genes using unbiased genome-wide functional genetic selection. Individual knockdown or cDNA overexpression of a set of 10 candidates reveals that most of these cell migration determinants are strongly dependent on the PI3K/PTEN/AKT pathway and on their downstream signals, such as FOXO1 and p70S6K1. ALK, one of the cell migration promoting genes, uniquely uses p55 γ regulatory subunit of PI3K, rather than more common p85 subunit, to trigger the activation of the PI3K-AKT pathway. Our method enables the rapid and cost-effective genome-wide selection of cell migration regulators. Our results emphasize the importance of the PI3K/PTEN/AKT pathway as a point of convergence for multiple regulators of cell migration.

¹Department of Pharmacology, Brain Science & Engineering Institute, BK21 Plus KNU Biomedical Convergence Program, Kyungpook National University School of Medicine, Daegu, Republic of Korea. ²College of Medicine, Dongguk University, Gyeongju, Republic of Korea. ³Korea Brain Research Institute (KBRI), Daegu, Republic of Korea. ⁴KNU Creative BioResearch Group, School of Life Sciences and Biotechnology, Kyungpook National University, Daegu, Republic of Korea. ⁵Laboratory of Molecular Carcinogenesis, National Institute of Environmental Health and Sciences, Research Triangle Park, North Carolina 27709, USA. ⁶Department of Genetics, Howard Hughes Medical Institute, Division of Genetics, Brigham and Women's Hospital, Harvard Medical School, Boston, Massachusetts 02115, USA. * These authors contributed equally to this work. Correspondence and requests for materials should be addressed to K.S. (email: ksuk@knu.ac.kr).

Cell migration is a dynamic process that requires coordinated cytoskeletal regulation and proper polarization, and is governed by the extracellular microenvironment, such as chemokines and growth factors. Cell migration is central to development, wound repair and tissue remodelling, and plays a major role in cancer metastasis^{1,2}. Cell migration to specific sites of inflammation or infection is also essential for immune system function, with respect to the elimination of foreign or infectious agents³. Given the relevance of cell migration in a variety of physiological and pathological conditions, we attempted to identify novel genes that regulate cell migration using the short hairpin RNA (shRNA)-based functional selection of cell migration phenotypes. Lentivirally delivered shRNAs were used to produce stable transcript knockdown in mouse fibroblast cells and to conduct loss of function genetic selections.

Genetic screening for genes that regulate cell migration and morphology has been previously performed in various invertebrate model organisms, such as, *Drosophila melanogaster* and *Caenorhabditis elegans*^{4,5}. The development of small interfering RNA (siRNA) and shRNA technology has also made it feasible to perform genetic screening in mammalian cells. siRNAs can be generated in organisms using shRNAs, consisting of a sequence of 21–29 nt, a short loop region, and the reverse complement of the 21–29 nt region⁶. shRNA libraries have been used to perform genetic screens in tissue culture cells for a variety of phenotypes⁷. Recent studies have analysed the closures of scratches in cellular monolayers after growth factor stimulation, using siRNA library targeting kinase and phosphatase genes^{8,9}. siRNA-based screening was performed to identify regulators of multiple cell adhesion complex formation¹⁰, and RNAi screening to identify inhibitors of cell migration using SKOV-3 cells (a highly motile ovarian carcinoma cell line)¹¹. More recently, new regulators of morphology, cytoskeletal organization and cell migration in human cells have been identified using genome-wide RNAi morphology screening data in *D. melanogaster* cells¹². Pooled shRNAs were also used for the genome-wide screen of cell migration regulators¹³, and, in that study, barcode microarray analysis was used to identify enriched shRNAs.

Herein, we adopted a selection and sequencing strategy to identify both cell migration-accelerating and -impairing genes using a genome-wide pooled shRNA library. Selection was performed using Boyden chamber assays followed by the separation and enrichment of cells with increased or decreased motility. shRNAs were then retrieved from selected cells and directly identified by half-hairpin barcode sequencing. This selection process resulted in the identification of 91 positive or negative regulators of cell migration; 29 of which genes had not been previously reported as cell migration regulators by RNAi screening. A set of 10 shRNAs was chosen for further validation studies, and these revealed remarkable dependences on the phosphoinositide-3 kinase (PI3K)/phosphatase and tensin homologue (PTEN)/AKT signalling pathway for cell migration acceleration or impairment.

Results

Genome-wide functional selection of cell migration regulators.

To identify novel cell migration-regulating genes, RNAi-based functional selection was performed. After introducing 63,996 pooled lentiviral mouse shRNAs targeting 21,332 genes into NIH3T3 mouse fibroblast cells, the shRNAs that accelerated or impaired baseline motility were selected using the transwell migration assay (Fig. 1a). Pooled recombinant lentivirus expressing shRNAs was generated by transfecting HEK293T cells with *pHAGE-mir30-RFP-shRNA* (targeting the mouse genome) (Fig. 1b), *pVSV-G*, *pTat*, *pPM2* and *pRev*. NIH3T3 fibroblast cells

were infected with the 63,996 pooled lentiviral mouse shRNA library at a multiplicity of infection (m.o.i.) of one^{14,15}. Two days after infection, shRNA-infected cells were selected with puromycin, placed into the upper compartment of a transwell unit and allowed to migrate through the perforated membrane to the lower compartment. Cells that exhibited accelerated or impaired migration were isolated from lower or upper compartments after 5 or 24 h of incubation, respectively; 5 and 24 h were chosen as optimal incubation times for these purposes (Supplementary Fig. 1). In fact, different cell types and assay conditions were used in the previous migration screens. These discrepancies in the experimental setups may determine the degree of agreement of the current results with published data (Supplementary Table 1). Cells with the desired phenotypes were enriched by repeating the procedure five times. After enrichment, genomic DNA was isolated, and shRNAs integrated into chromosomes were retrieved by PCR amplification, cloned and sequenced. The determined sequences of half-hairpin barcode were used to identify the shRNAs. This selection method identified 91 shRNAs that accelerated or impaired migration (Tables 1 and 2). Sixty-two of the 91 identified target genes have been previously associated with cell migration by RNAi screen^{8–10,13,16} (Supplementary Tables 2 and 3). The remaining 29 target genes had not been previously identified as cell migration regulators by RNAi screen. To determine relationships between cell migration regulators, a signalling network was built by ingenuity pathway analysis (IPA) analysis (Fig. 2). This analysis revealed that the newly identified cell migration regulators were closely linked to various cell movement signalling components (Fig. 2a). The 91 cell migration-regulating genes identified were mapped to several major biological functions by IPA analysis; these functions included cell movement and morphology (41%), cellular assembly and organization (21%), cell-to-cell signalling (20%), and protein trafficking and molecular transport (18%) (Fig. 2b). Functional sub-networks were also constructed based on the biological functions in which they participate (Supplementary Fig. 2a–d). Sub-network topology indicated a close interaction between the newly identified cell migration regulators and various functional components. Direct or indirect protein–protein interactions were also found between the identified regulators and other cell migration signalling components (Supplementary Fig. 2e). Several additional targets were identified, not found in the primary selection, which might be predicted to modulate cell migration through network inference; these include CTNNB1, CDK4, MYC, IRS4, EIF3F, KIF5C and so on. In addition, a partial cell migration network was constructed, based on signalling pathways initiated by growth factor/receptor tyrosine kinase, fibronectin/integrin or chemotactic factor/GPCR (Supplementary Fig. 2f). Many nodes in the network were candidate genes identified in the current selection. PI3K, PTEN and AKT emerged as convergent points in multiple networks. This result was not surprising, as the PI3K/AKT axis is known to regulate cell migration under diverse conditions. In addition, subcellular localization and disease association of the cell migration-regulating genes were analysed (Supplementary Fig. 3 and Supplementary Tables 4 and 5). The majority of the genes were associated with cancer and neurological diseases.

Validation of selected cell migration regulators. Among the 91 shRNAs identified (Tables 1 and 2), 10 were selected for further investigation (Supplementary Table 6). These shRNAs were selected, as little or no evidence linked the corresponding target genes with the regulation of cell migration. shRNA-induced phenotypes were validated using siRNA-mediated knockdown.

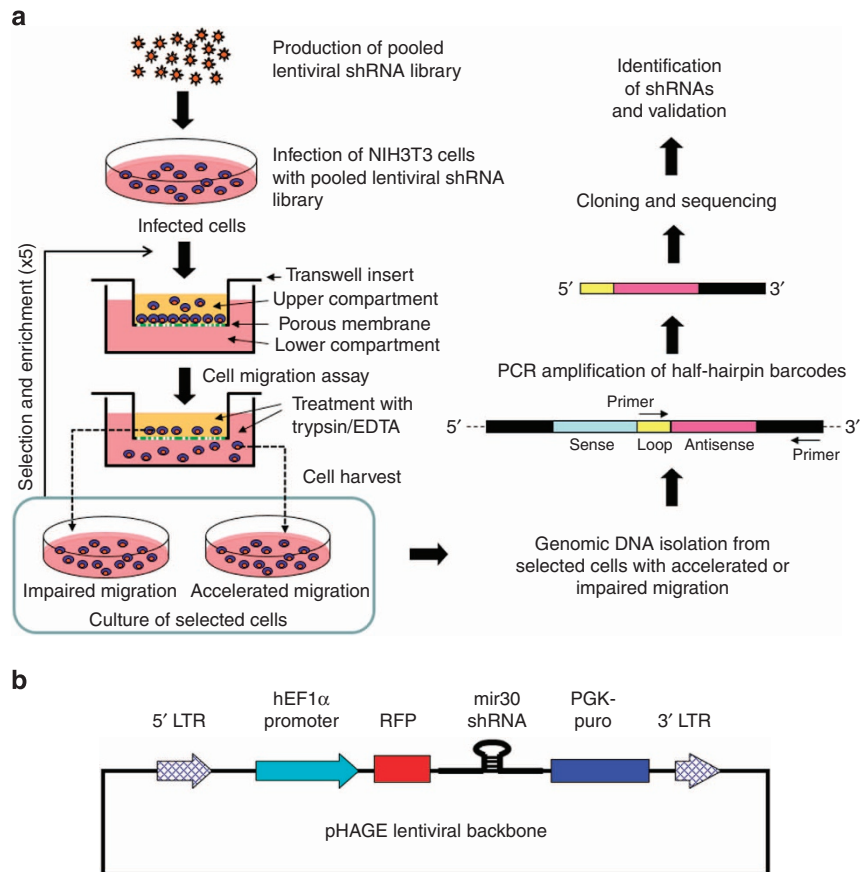


Figure 1 | Schematic representation of the RNAi-based selection of cell migration regulators. (a) Overview of the selection procedure. The production and infection of genome-wide lentiviral shRNA library are described in Methods. Two days after lentiviral infection, NIH3T3 mouse fibroblast cells were seeded onto transwell inserts and allowed to migrate across the porous membrane at 37 °C for 5 or 24 h, to select cells with an increased or decreased migration phenotype, respectively. Migrated or non-migrated cells were collected by trypsin-EDTA treatment from the lower or upper faces, respectively, of inserts, and reseeded onto transwell culture inserts for a second round of selection (this process was repeated five times). After the final round of selection, shRNAs were retrieved by PCR from selected cells and identified by sequencing. **(b)** Diagram of pHAGE-mir30-RFP-shRNA vector. The pooled lentiviral vector contained 63,996 different mir30-based shRNAs targeting 21,332 mouse genes.

To avoid off-target effects, five siRNA duplexes were synthesized for each shRNA candidate identified. Targeting sequences of the siRNAs were distinct from those of the shRNA constructs. The wound-healing assay revealed that transfection with the siRNAs of five migration-accelerating shRNA candidates (*mtmr1*, *lats2*, *dock3*, *myo5a* and *ptpn14*) (Fig. 3a,b) or with the siRNAs of five migration-impaired shRNA candidates (*csnk2a2*, *arid4a*, *ppp3cc*, *irf4* and *alk*) (Fig. 3c,d) increased or decreased, respectively, the motility of NIH3T3 fibroblast cells as compared with control siRNA transfectant. The cell migration-regulating activities of these candidates were also examined using the transwell migration assay, and similar results were obtained (Fig. 4a,b). In addition, the cell migration-regulating activities of these candidates were confirmed in L929 mouse fibroblast and mouse embryonic fibroblast (MEF) cells using the transwell migration assay, which indicated that the observed cell migration-regulating effects of the siRNAs were not limited to a single cell line (Fig. 4c,d). siRNA-mediated knockdown of the 10 target genes mentioned above was confirmed by RT-PCR (Fig. 3b,d), and >50% knockdown was achieved for all siRNAs tested. siRNA-mediated knockdown of the target genes was also confirmed at the protein levels by western blot analysis (Supplementary Fig. 4a–e). Furthermore, it should be noted that the cell migration-regulating properties of siRNAs in the wound-healing assay and transwell migration assay were not due to effects on cell

proliferation, as determined by MTT assay (Supplementary Fig. 4f–h). Validation experiments were extended to other hits identified in the selection and network-derived candidates. Additional 36 hits (20 migration-accelerating shRNAs and 16 migration-impaired shRNAs) and four network-derived candidates (*ctnnb1*, *cdk4*, *myc* and *irs4*) were tested using pooled retroviral shRNAs (Supplementary Table 7, Supplementary Fig. 5 and Supplementary Movies 1–3). As a result, 71.7% (33/46) of the hits showed cell migration-regulating activity consistent with the primary screen. Among the four network-derived candidates, *ctnnb1* and *cdk4* shRNAs promoted and inhibited cell migration, respectively, thereby demonstrating 50% validation for the network analysis.

Common roles of the PI3K/PTEN/AKT pathways. Network analysis of the cell migration regulators identified indicated that the PI3K/PTEN/AKT signalling pathway plays a central role (Fig. 2 and Supplementary Fig. 2). PI3K/PTEN/AKT signalling has been previously associated with cell migration. For example, PI3K/AKT has been reported to enhance actin remodelling, to generate membrane protrusions and to induce cell migration and cell invasion via remodelling of the actin cytoskeleton¹⁷. PTEN is a lipid phosphatase that dephosphorylates the D3 position of phosphatidylinositol-3,4,5-trisphosphate (PIP3), a

Table 1 | List of shRNAs that accelerated cell migration (with targets genes inhibiting cell migration).

Symbols	Target genes	GenBank accession No.
<i>Cell cycle</i>		
<i>dgkz</i>	Diacylglycerol kinase zeta	NM_138306
<i>Cell morphology</i>		
<i>dock3</i>	Dedicator of cyto-kinesis 3	NM_153413
<i>myo5a</i>	Myosin VA	NM_010864
<i>Cell signalling</i>		
<i>ppid</i>	Peptidylprolyl isomerase D (cyclophilin D)	NM_026352
<i>Cellular development</i>		
<i>acvr1</i>	Activin A receptor, type 1	NM_007394
<i>cdk13</i>	Cyclin-dependent kinase 13	NM_027118
<i>Inflammatory response and disease</i>		
<i>enpp2</i>	Ectonucleotide pyrophosphatase/phosphodiesterase 2	NM_001136077
<i>gfra2</i>	Glial cell line derived neurotrophic factor family receptor alpha 2	NM_008115
<i>icam2</i>	Intercellular adhesion molecule 2	NM_010494
<i>lats2</i>	Large tumour suppressor 2	NM_015771
<i>Inflammatory response and disease</i>		
<i>ptpn14</i>	Protein tyrosine phosphatase, non-receptor type 14	NM_008976
<i>h2-Q10</i>	Histocompatibility 2, Q region locus 10	BC042572
<i>Molecular transport</i>		
<i>pcyt1a</i>	Phosphate cytidylyltransferase 1, choline, alpha isoform	NM_009981
<i>pts</i>	6-pyruvoyl-tetrahydropterin synthase	NM_011220
<i>Post-translational modification</i>		
<i>sbf2</i>	SET-binding factor 2	NM_177324
<i>Other/unknown</i>		
<i>A930006J02Rik</i>	RIKEN cDNA A930006J02 gene	AK020818
<i>atmin</i>	ATM interactor	NM_177700
<i>cntnap4</i>	Contactin-associated protein-like 4	NM_130457
<i>coro1b</i>	Coronin, actin-binding protein 1B	NM_011778
<i>D630033O11Rik</i>	RIKEN cDNA D630033O11 gene	XM_001001707
<i>gabra4</i>	Gamma-aminobutyric acid A receptor, subunit alpha 4	NM_010251
<i>gm379</i>	Gm379-predicted gene 379	XM_142052
<i>gm1971</i>	Gm1971-predicted gene 1971	XM_001472879
<i>gm5615</i>	Predicted gene 5615	NM_001033783
<i>gm12273</i>	Gm12273 predicted gene 12273	XM_001479118
<i>gnal</i>	Guanine nucleotide-binding protein, alpha stimulating, olfactory type	NM_010307
<i>gpkow</i>	G patch domain and KOW motifs	NM_173747
<i>itpril2</i>	Inositol 1,4,5-triphosphate receptor-interacting protein-like 2	NM_001033380
<i>lair1</i>	Leukocyte-associated Ig-like receptor 1	NM_001113474
<i>LOC668961</i>	LOC668961 spindlin 2 family member	XM_001006595
<i>mia3</i>	Melanoma inhibitory activity 3	NM_177389
<i>mpc1</i>	Mitochondrial pyruvate carrier 1	NM_018819
<i>mtmr1</i>	Myotubularin related protein 1	NM_016985
<i>otud6b</i>	OTU domain containing 6B	NM_152812
<i>ptpn3</i>	Protein tyrosine phosphatase, non-receptor type 3	NM_011207
<i>ptpn23</i>	Protein tyrosine phosphatase non-receptor type 23	NM_001081043
<i>ptx4</i>	Pentraxin 4	NM_001163416
<i>rfp14</i>	Ret finger protein-like 4	NM_138954
<i>trim59</i>	Tripartite motif-containing 59	NM_025863
<i>trip10</i>	Thyroid hormone receptor interactor 10	NM_134125
<i>usp45</i>	Ubiquitin specific peptidase 45	NM_152825
<i>zbed3</i>	Zinc-finger, BED domain containing 3	NM_028106

shRNAs were categorized by biological function using DAVID (database for annotation, visualization and integrated discovery).

second messenger produced by PI3K and that activates AKT^{18,19}. PTEN is also known to antagonize the cell migration-promoting activity of PI3K. To determine whether the PI3K/PTEN/AKT signalling pathway is involved in the accelerated or impaired migration induced by shRNAs, we first assessed AKT phosphorylation after knocking down *dock3*, *mtmr1*, *ptpn14*, *lats2* and *myo5a*, and after overexpressing *alk* and *irf4*. A knockdown of *dock3*, *mtmr1*, *ptpn14* or *myo5a*, but not of *lats2*, or the overexpression of *alk* or *irf4* induced the phosphorylation of AKT (Fig. 5a–c). The overexpression of *alk* or *irf4* in transfectants was confirmed by western blot analysis (Fig. 5d). In addition, we used pharmacological inhibitors of PI3K or AKT

to evaluate the role of PI3K/AKT signalling in the accelerated or impaired cell migration by shRNAs. siRNA-mediated knockdown was done to upregulate cell migration for cell migration-inhibiting genes, whereas cDNA overexpression was done to upregulate cell migration for cell migration-promoting genes. The accelerated cell migration observed after *mtmr1*, *dock3*, *myo5a* or *ptpn14* (but not *lats2*) knockdown was significantly attenuated by AKT or PI3K inhibitors in the wound-healing (Fig. 6a) and transwell assays (Fig. 7a). Similarly, the accelerated cell migration observed for *alk* or *irf4* overexpression was also attenuated by these inhibitors in the wound-healing (Fig. 6b) and transwell assays (Fig. 7b). Taken together, these results indicate that the cell

Table 2 | List of shRNAs that impaired cell migration (with targets genes promoting cell migration).

Symbols	Target genes	GenBank accession No.
<i>Cell cycle</i>		
<i>clip1</i>	CAP-GLY domain containing linker protein 1	NM_019765
<i>Cell morphology</i>		
<i>actg1</i>	Actin, gamma, cytoplasmic 1	NM_009609
<i>add1</i>	Adducin 1 (alpha)	NM_001024458
<i>akt3</i>	V-akt murine thymoma viral oncogene homologue 3 (protein kinase B, gamma)	NM_011785
<i>des</i>	Desmin	NM_010043
<i>itgb8</i>	Integrin beta 8	NM_177290
<i>pik3ca</i>	Phosphoinositide-3-kinase, catalytic, alpha polypeptide	NM_008839
<i>rdx</i>	Radixin	NM_009041
<i>sep15</i>	Selenoprotein	NM_053102
<i>sorbs1</i>	Sorbin and SH3 domain containing 1	NM_001034962
<i>tpm3</i>	Tropomyosin 3,gamma	NM_022314
<i>vim</i>	Vimentin	NM_011701
<i>Cell signalling</i>		
<i>apc</i>	Adenomatosis polyposis coli	NM_007462
<i>Cellular assembly and organization</i>		
<i>adam2</i>	A disintegrin and metallopeptidase domain 2	NM_009618
<i>Cellular development</i>		
<i>alk</i>	Anaplastic lymphoma kinase (Ki-1)	NM_007439
<i>irf4</i>	Interferon regulatory factor 4	NM_013674
<i>igf1r</i>	Insulin-like growth factor 1 receptor	NM_010513
<i>Cellular movement</i>		
<i>abl1</i>	V-abl Abelson murine leukemia viral oncogene homologue 1	NM_009594
<i>abl2</i>	V-abl Abelson murine leukemia viral oncogene homologue 2 (arg, Abelson-related gene)	NM_001136104
<i>arhgap5</i>	Rho GTPase activating protein 5	NM_009706
<i>csnk1a1</i>	Casein kinase 1, alpha 1	NM_146087
<i>csnk2a2</i>	Casein kinase 2, alpha prime polypeptide	NM_009974
<i>irgm1</i>	Immunity-related GTPase family M member 1	NM_008326
<i>itgav</i>	Integrin, alpha V (vitronectin receptor, alpha polypeptide, antigen CD51)	NM_008402
<i>nrp2</i>	Neuropilin 2	NM_001077403
<i>pak4</i>	p21 protein (Cdc42/Rac)-activated kinase 4	NM_027470
<i>Metabolism</i>		
<i>abi2</i>	Abl interactor 2	NM_001198570
<i>mogat1</i>	Monoacylglycerol O-acyltransferase 1	NM_026713
<i>Other/unknown</i>		
<i>akap11</i>	A kinase (PRKA) anchor protein 11	NM_001164503
<i>arhgap26</i>	Rho GTPase activating protein 26	NM_175164
<i>arid4a</i>	AT rich interactive domain 4A (RBP1-like)	NM_001081195
<i>ccdc34</i>	Coiled-coil domain containing 34	NM_026613
<i>cdc42</i>	Cell division cycle 42 (GTP binding protein, 25 kDa)	NM_009861
<i>cdh12</i>	Cadherin 12, type 2 (N-cadherin 2)	NM_001008420
<i>cmtm2b</i>	CKLF-like MARVEL transmembrane domain containing 2B	NM_028524
<i>defb20</i>	Defensin beta 20	NM_176950
<i>eif3e</i>	Eukaryotic translation initiation factor3, subunit E	NM_008388
<i>frmd6</i>	FERM domain containing 6	NM_028127
<i>g3bp2</i>	Ras-GTPase activating protein SH3 domain-binding protein 2	NM_001080794
<i>gpr143</i>	G protein-coupled receptor 143	NM_010951
<i>hpd1</i>	4-hydroxyphenylpyruvate dioxygenase-like	NM_146256
<i>hsd17b11</i>	Hydroxysteroid (17-beta) dehydrogenase 11	NM_053262
<i>pdgfr1</i>	Platelet-derived growth factor receptor-like	NM_026840
<i>ppp3cc</i>	Protein phosphatase 3, catalytic subunit, gamma isoform	NM_008915
<i>mf139</i>	Ring finger protein 139	NM_175226
<i>rp17</i>	Ribosomal protein L7	NM_011291
<i>stradb</i>	STE20-related kinase adaptor beta	NM_172656
<i>svil</i>	Supervillin	NM_178046
<i>tm4sf5</i>	Transmembrane 4 superfamily member 5	NM_029360

shRNAs were categorized by biological function using DAVID (database for annotation, visualization and integrated discovery).

migration promoters (*csnk2a2*, *arid4a*, *irf4* and *alk*) and the inhibitors (*mtmr1*, *dock3*, *myo5a* and *ptpn14*) mediate their effects via the PI3K/AKT pathway. Furthermore, at the concentration used in the current study, the PI3K and AKT inhibitors effectively inhibited downstream signalling pathways and were without effects on cell viability (Supplementary Fig. 6). To gain a better understanding of the role of PI3K/AKT signalling

in cell migration following specific gene knockdown, *foxo1* and *p70s6k1* (downstream components of the AKT pathway) were investigated. The phosphorylation of FOXO1 and p70S6K1 was increased after knockdown of the migration-inhibiting genes *dock3*, *mtmr1*, *ptpn14* and *myo5a*, and after the upregulation of the migration-promoting genes (*alk* and *irf4*) (Supplementary Fig. 7). These results support that activation of the PI3K/AKT

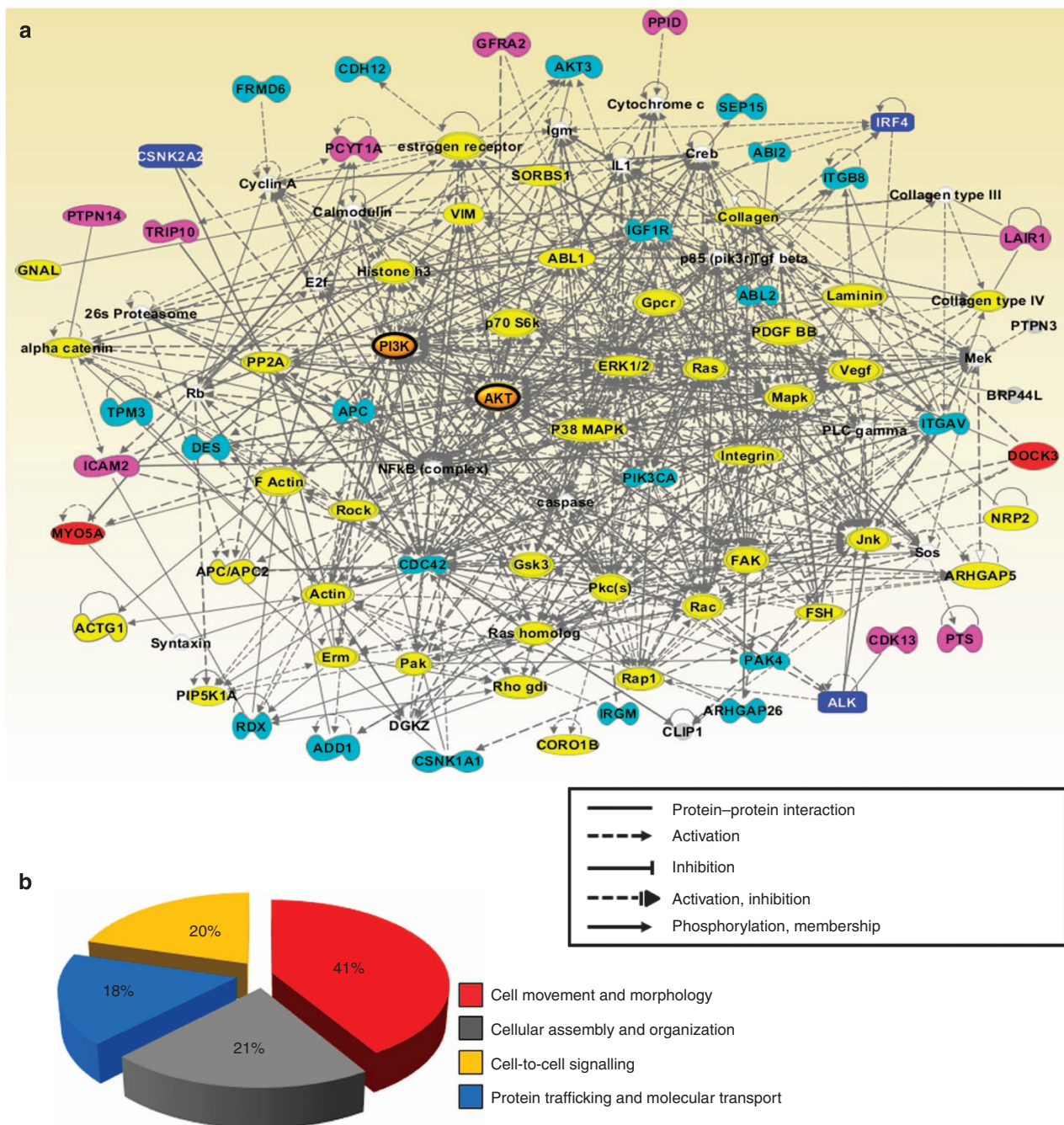


Figure 2 | Construction of the signalling network of cell migration regulators and their classification based on biological functions. (a) A relevant signalling network was constructed from the 91 cell migration-regulating genes identified by ingenuity pathway analysis (IPA). Newly identified cell migration regulators were linked to various previously reported cell movement signalling components (yellow). Green, cell migration-accelerating genes; blue, cell migration-accelerating genes validated by siRNA; pink, cell migration-impairing genes; red, cell migration-impairing genes validated by siRNA study. PI3K and AKT are highlighted in brown. (b) The biological functions of cell migration regulators were categorized by IPA analysis, which showed 41% were cell movement and morphology related, 21% were cellular assembly and organization related, 20% were cell-to-cell signalling related and 18% were protein trafficking and molecular transport related.

pathway and downstream events, such as FOXO1 and p70S6K1 phosphorylation, appear to be critically required for diverse cell migration regulators identified by unbiased functional selection.

Unique role of p55 γ regulatory subunit of PI3K. In the next set of experiments, the cell migration-promoting gene *alk* was subjected to further investigation. Many receptor tyrosine kinases

transduce their signals via specific interactions with SH2 domain-containing proteins such as regulatory subunits of PI3K²⁰. Therefore, we asked whether the receptor tyrosine kinase *alk* regulates the PI3K pathway through interaction with regulatory subunits of PI3K. Although anaplastic lymphoma kinase (ALK) physically interacted with both p85 α and p55 γ regulatory subunits of PI3K (Fig. 8a,b), ALK overexpression enhanced phosphorylation of p55 γ , but not p85 α , subunit (Fig. 8c). The

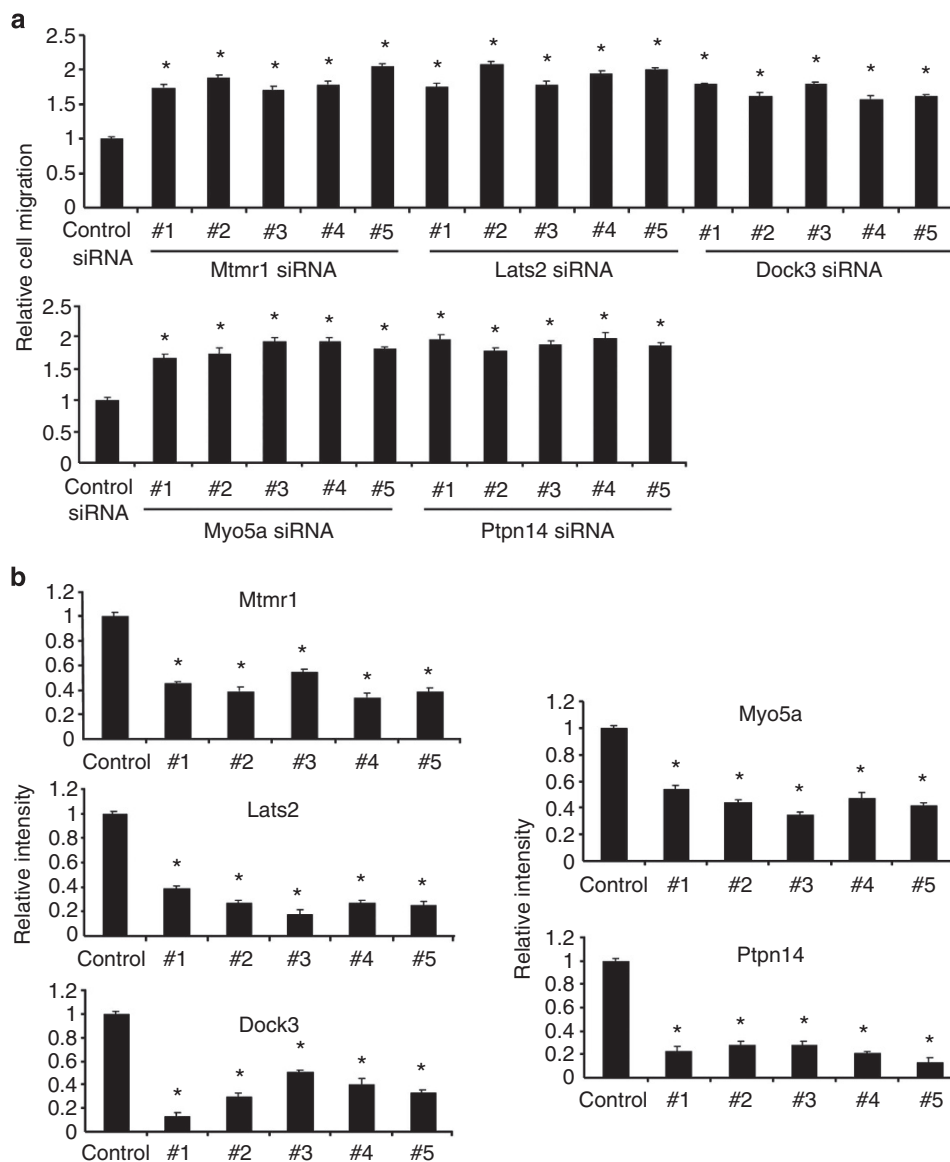


Figure 3 | Validation of the gene targets found by the RNAi-based functional selection. (a) NIH3T3 fibroblast cells were transiently transfected with control siRNA or one of five siRNAs (#1 to #5) targeting *mtmr1*, *lats2*, *dock3*, *myo5a* or *ptpn14*. At 24 h after transfection, wound-healing assays were performed to evaluate cell migration. (b) Efficiencies of siRNA-mediated target gene knockdown were confirmed by RT-PCR followed by densitometric analysis. (c) NIH3T3 cells were transiently transfected with control siRNA or one of five siRNAs (#1 to #5) for each target gene identified (*csnk2a2*, *arid4a*, *ppp3cc*, *irf4* and *alk*). After 24 h, wound-healing assays were performed to evaluate cell migration. Cell migration was quantified by measuring degrees of wound closure, as described in Methods. The results shown are means \pm s.d. ($n=3$). $*P<0.05$ represents significantly different from control siRNA-transfected cells. (d) Efficiencies of siRNA-mediated target gene knockdown were confirmed by RT-PCR and densitometric analysis. β -Actin was used as the internal control. The results are mean \pm s.d. ($n=3$); $*P$ -values of <0.05 indicate significantly different from control siRNA-transfected cells.

ALK-induced phosphorylation of p55 γ regulatory subunit of PI3K was accompanied by AKT phosphorylation (Fig. 8c) and translocation to the plasma membrane (Fig. 8d). GFP-fused AKT-PH domain was used to demonstrate the membrane translocation of AKT²¹. The critical role of p55 γ and its phosphorylation in AKT activation and subsequent cell migration was further evaluated by siRNA-mediated knockdown of p55 γ (Fig. 8e,f and Supplementary Fig. 8)²². p55 γ siRNAs decreased ALK-induced AKT phosphorylation and cell migration, further supporting the unique role of p55 γ subunit of PI3K in the Alk-promoted cell migration. These results indicate that ALK promotes cell migration by specifically interacting with p55 γ subunit of PI3K, rather than more common p85 subunit (Supplementary Fig. 9a).

Discussion

We utilized lentivirus-based shRNA libraries targeting the entire mouse genome to enable genome-wide loss-of-function analysis by stable gene knockdown. Broad application of this shRNA library has already been reported in numerous studies on the identification of human disease-related genes^{23–28} and genes associated with other phenotypes of interest^{29–33}. In the current study, we aimed to identify diverse cellular pathways whose knockdowns have positive or negative effects on cell migration phenotypes. Some of the cell migration-regulating genes identified in the present study have well-established links to cellular motility, which validates the selection approach used. We also identified a number of previously uncharacterized cell migration regulators not previously identified by RNAi

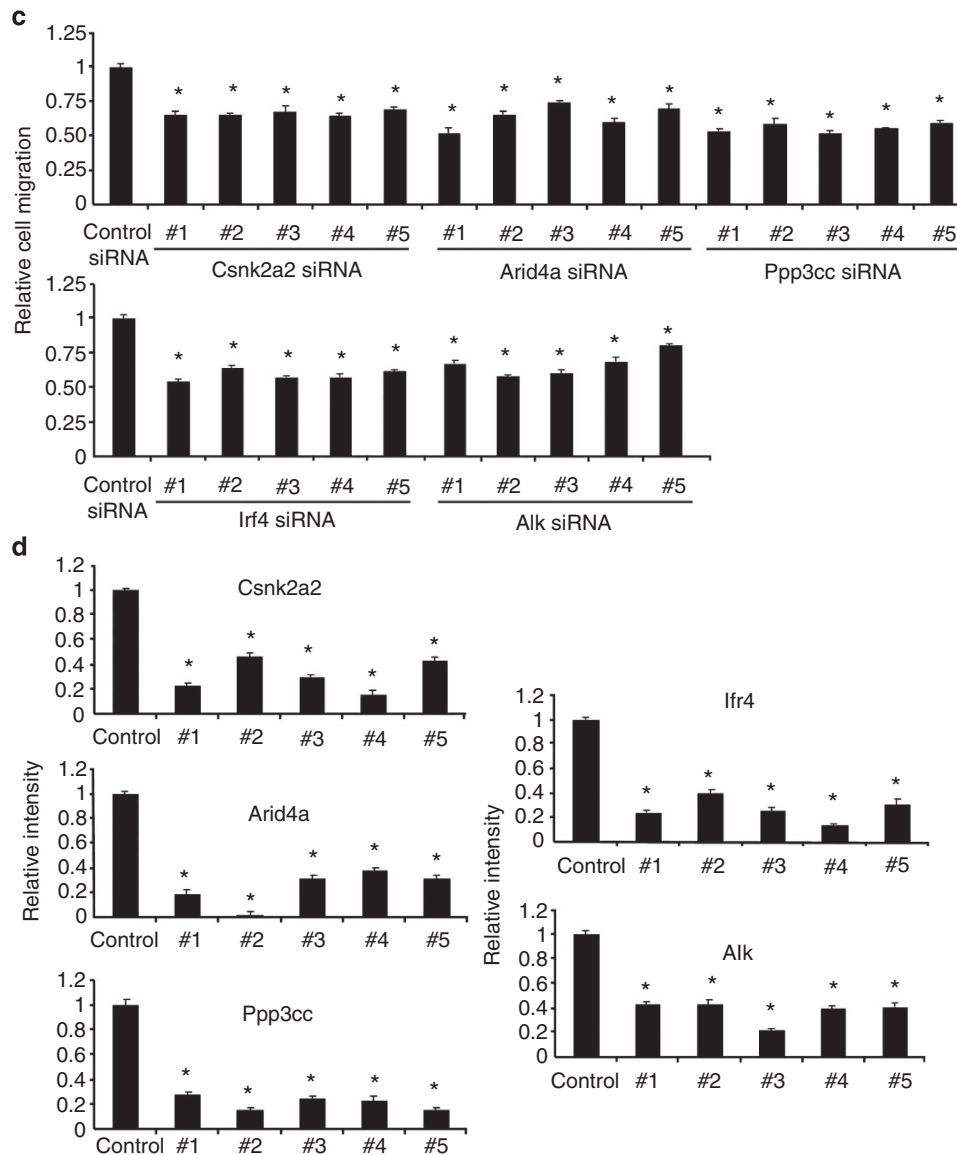


Figure 3 | Continued.

screening. Importantly, several novel cell migration regulators that were investigated in more detail were found to show marked downstream signalling convergence on the PI3K/PTE/AKT pathway, which emphasizes the central roles of this pathway in cell migration.

Although the RNAi-based functional screening of cell migration regulators has been previously conducted, our approach differs in several ways. First, we performed unbiased genome-scale shRNA selection, rather than screening, as phenotype-driven selection processes reduce false positives and as cells with given phenotypes are separated and enriched several times. The selection method used in the present study is straightforward and cost-effective as compared with array-based RNAi screen. Second, we used cells of fibroblast origin, which have higher baseline motilities than epithelial cells, as this allowed us to select cell migration accelerators and impairers at the same time. In the event, the selection method used identified many migration-promoting and -inhibiting genes not previously reported. Third, we used direct cloning and sequencing of half-hairpin barcodes, rather than microarray analysis, to identify selected shRNAs. This process enabled the unbiased and direct selection of genes

contributing to a given phenotype, as microarray-based identification involves statistical evaluation and a degree of ambiguity. In this method, however, it was difficult to assess how representative the selected shRNAs are to the starting shRNA library.

Among the functionally diverse 91 hits identified in the primary screen, targets of 13 shRNAs were protein kinases and protein phosphatases. Our results support the validity of the selection methods used and emphasize the critical roles played by protein kinases and phosphatases in cell motility regulation. Some of these kinases and phosphatases were included in our initial validation list, which comprised five migration-accelerating shRNA candidates (*mtmr1*, *lats2*, *dock3*, *myo5a* and *ptpn14*) and five migration-impairing shRNA candidates (*csnk2a2*, *arid4a*, *ppp3cc*, *irf4* and *alk*). In later studies, we found that the actions of some of these cell migration regulators, namely, *mtmr1*, *dock3*, *myo5a*, *ptpn14*, *csnk2a2*, *alk*, *irf4* and *arid4a* (but not *lats2* or *ppp3cc*), are strongly dependent on the PI3K/PTE/AKT pathway (Supplementary Fig. 9b). Additional validation studies of 36 hits showed 71.7% overall correlation between the results of primary screen and secondary test.

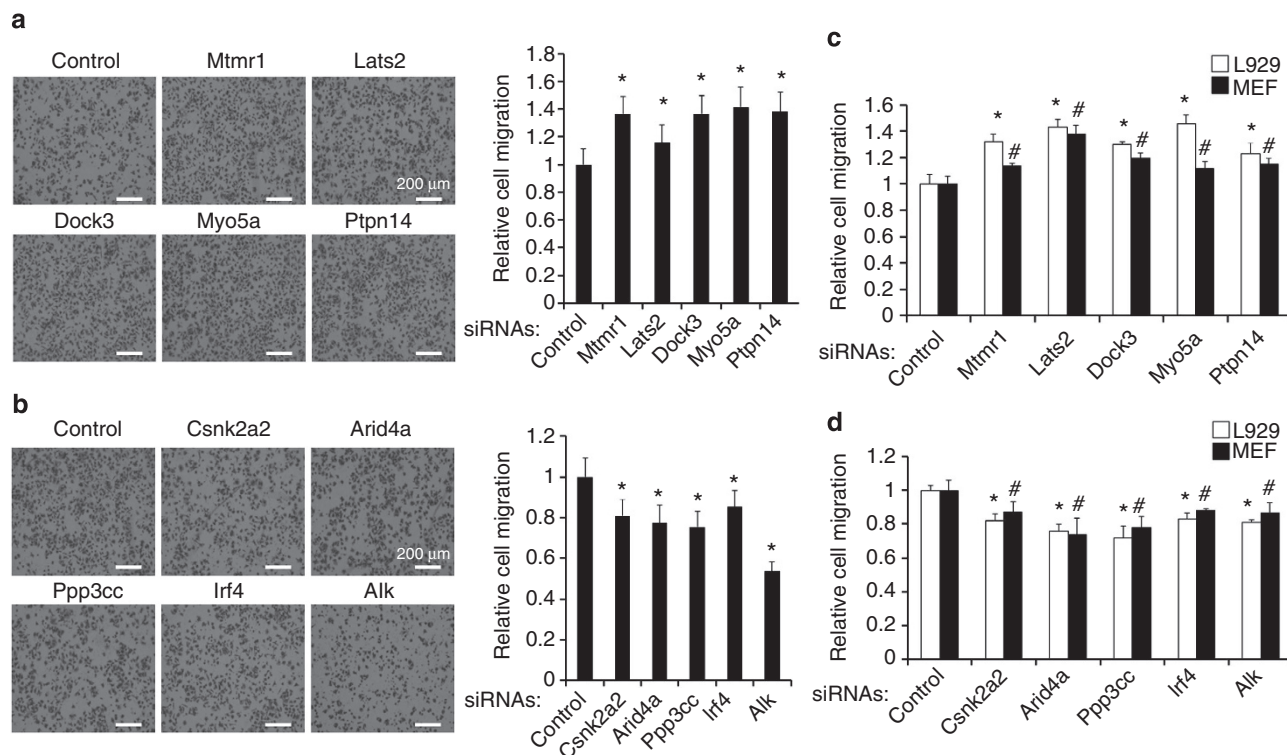


Figure 4 | Validation of shRNA hits by three-dimensional cell migration assay. (a,b) NIH3T3 fibroblast cells were transiently transfected with siRNAs targeting cell migration inhibitors (a) or promoters (b). One siRNA was used for each target: *mtmr1* (#5), *lats2* (#3), *dock3* (#1), *myo5a* (#3), *ptpn14* (#5), *csnk2a2* (#1), *arid4a* (#1), *ppp3cc* (#3), *irf4* (#4) or *alk* (#3). #1 to #5 indicate the siRNAs used for validation in Fig. 3. After 24 h of transfection, NIH3T3 fibroblast cells (4×10^4 cells/well) were seeded onto transwell inserts and incubated at 37 °C for 6 h (a; cell migration-accelerating siRNAs) or 9 h (b; cell migration-impairing siRNAs). Non-migrated cells were removed from the upper face of the transwell insert using a cotton swab. Cells that migrated through membranes were stained and counted in five randomly selected fields. The results are representative of three independent experiments (left) or mean \pm s.d. ($n=3$) (right). * $P < 0.05$ represents significantly different from control siRNA-transfected NIH3T3 cells. Scale bar, 200 μ m. (c,d) L929 fibroblast cells or mouse embryonic fibroblasts (MEFs) were transiently transfected with cell migration-accelerating (c) or impairing (d) siRNAs identified from the screen. After 24 h of transfection, L929 or MEF cells (4×10^4 cells/well) were seeded onto the transwell culture inserts and incubated at 37 °C for 6–9 h. After incubation, non-migrated cells were removed from the upper face of the transwell culture insert using a cotton swab. The cells that migrated across the membrane were stained and counted as described in the main text. The results are mean \pm s.d. ($n=3$). * $P < 0.05$ represents significantly different from control siRNA-transfected L929 cells. # $P < 0.05$ represents different from control siRNA-transfected MEF cells.

Several of the cell migration-regulating genes identified in this study have been previously associated with the PI3K/PTEEN/AKT pathway. Casein kinase 2 (CK2 or *csnk2*) is a physiologically relevant PTEEN kinase, and CK2-mediated phosphorylation inhibits PTEEN function, which in turn increases PIP3 levels, and thus AKT phosphorylation. The expression levels and activities of CK2 subunits have been reported to be increased three- to fivefold in many human cancer and tumour cell lines^{34–36}. Protein tyrosine phosphatase non-receptor type 14 (*ptpn14*) is frequently mutated in a variety of human cancers. However, the cell signalling pathways regulated by Ptpn14 remain largely unknown³⁷. In the present study, protein–protein interaction between PTPN14 and PTEEN was identified by IPA analysis (Supplementary Fig. 2e), which suggests that PTPN14 regulates cell migration by modulating PTEEN activity. The physiological role of myotubularin-related protein 1 (*mtmr1*) has not been clearly determined, although recent studies have shown that *mtmr1* is a phosphatase, like myotubularin, and can dephosphorylate both PtdIns3P and PtdIns3,5P2 *in vitro*^{38,39}, which suggests its possible involvement in the PI3K/PTEEN/AKT pathway.

Some of the cell migration regulators identified in this study appear to act independently of the PI3K/PTEEN/AKT pathway. *Ppp3cc*, also known as calcineurin A subunit, is a Ca²⁺- and calmodulin-dependent serine/threonine protein phosphatase. In a

recent study, calcineurin was shown to promote tumour cell invasion via transcriptional factor NFAT in breast cancer metastasis⁴⁰. *Lats2* is a serine/threonine protein kinase belonging to the tumour suppressor family, and has been reported to participate in p53 signalling⁴¹ and to be implicated in cell cycle regulation, apoptosis, centrosome duplication and genomic stability^{42–44}. Furthermore, our findings suggest that both *ppp3cc* and *lats2* promote or inhibit cell migration, respectively, via a mechanism not involving the PI3K/PTEEN/AKT pathway.

In the present study, the activations of FOXO1 and p70S6K1 were investigated as signalling events downstream of the PI3K/PTEEN/AKT pathway to determine the mechanistic basis of impaired or accelerated cell migration following specific gene knockdown. Forkhead box O (FOXO) proteins, which include FOXO1, FOXO3, FOXO4 and FOXO6, regulate many cancer-related phenotypes by inhibiting nuclear transcription factors. In the previous studies, activation of AKT led to FOXO1 phosphorylation and nuclear exclusion⁴⁵. Furthermore, the nuclear exclusion of FOXO1 abolishes its inhibitory effect on Runx2 activity, and therefore enhances Runx2-mediated gene transcription and the subsequent migration/invasion of cancer cells⁴⁶. In addition, the AKT-mediated phosphorylation of FOXO1 induces its degradation by proteasome^{47,48}. Consistent

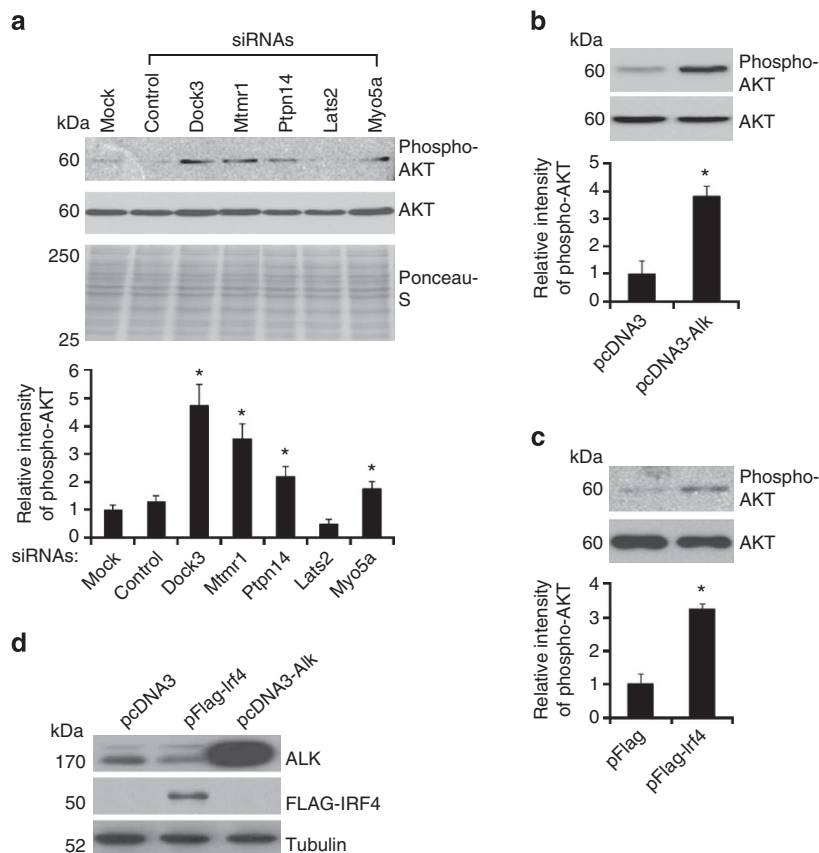


Figure 5 | Induction of AKT activation by the selected cell migration regulators. NIH3T3 fibroblast cells were transiently transfected with control siRNA, siRNAs against *dock3* (#1), *mtmr1* (#5), *ptpn14* (#5), *lats2* (#3) or *myo5a* (#3) (**a**) or empty vectors (*pcDNA3* or *pFlag*), *alk* or *irf4* expression constructs (*pcDNA3-alk* or *pFlag-irf4*) (**b,c**). After 48 h, levels of phosphorylated AKT (phospho-AKT at Ser473) or total AKT protein were evaluated by western blot analysis (upper). Ponceau S staining was performed to confirm equal sample loading. The results of densitometric analysis are also shown (lower). The results shown are means \pm s.d. ($n = 3$); * P -values of < 0.05 indicate significantly different from control siRNA- or empty vector-transfected cells. (**d**) Overexpression of ALK or IRF4 in transfectants was confirmed by western blotting using an anti-ALK or -FLAG-tag antibody. Tubulin was used as the internal control.

with previous findings, we found that the level of FOXO1 was reduced after phosphorylation (Supplementary Fig. 7). In a previous study, mTORC1 and mTORC2 signalling pathways were found to be involved in cytoskeletal rearrangement and cell migration^{49,50}. In particular, the activations of mTORC1 and p70S6K1 were found to be essential for the migration and invasion of cancer and non-cancer cells via cytoskeletal rearrangement^{49,51}. In the present study, the phosphorylation of AKT, FOXO1 and p70S6K1 was found to be associated with increased cell migration, which supports the notion that FOXO1 and p70S6K1 are downstream signalling components of PI3K/PTEN/AKT.

The PI3K family is categorized into three classes (class I, II, and III) and various subclasses based on their structure, substrate specificity and regulation. The class I PI3K is the best-characterized subfamily present in all cell types. They consist of a p110 catalytic subunit (α , β , γ or δ) and a regulatory subunit (p85 α , p85 β , p55 α , p55 γ or p50 α)⁵². Regulatory subunits are required to recruit the p110 catalytic subunit to specific cellular locations, thereby regulating its catalytic activity. The different regulatory subunits associate with distinct receptor tyrosine kinases⁵³ and show the specificity in mediating different PI3K signalling pathways⁵⁴. However, the mechanisms by which these regulatory subunits regulate specific signalling pathways are not fully understood. p55 γ , also known as p55PIK, binds the catalytic subunits and modulates PI3K activity in a manner similar to p85 α

and p85 β ^{54,55}. Our data indicate that p55 γ was critically involved in the receptor tyrosine kinase Alk-promoted PI3K/AKT activation and cell migration. In the previous reports, p55 γ regulatory subunit of PI3K promoted cell cycle progression⁵⁶, DNA synthesis⁵⁷, proliferation and differentiation of leukemia cells⁵⁸, and tumour angiogenesis via regulation of NF- κ B signalling or expression of VEGF-A⁵⁹. Furthermore, the protein levels of p55 γ increased in colorectal, gastric and ovarian cancers^{56,59,60}. PI3K also plays an important role in the multiple steps of neurite outgrowth during nerve growth factor-stimulated differentiation and in the brain development⁶¹.

ALK was originally identified as an oncogene in human anaplastic large cell lymphoma and neuroblastoma⁶². ALK displays the classical structural features of a receptor tyrosine kinase. In the previous studies, ALK mediated several signal-transduction pathways, including JAK/STAT, RAS/MAPK, PI3K and PLC γ , and modulated various cellular functions, such as proliferation, angiogenesis, metabolism and migration^{63,64}. An important role of ALK in the development and function of the nervous system has also been reported⁶⁵. Brain expression of ALK changed during mouse⁶⁶ or zebrafish⁶⁷ embryogenesis, consistent with our results. However, little is known about physiological functions of ALK and its cognate ligands in vertebrate. In this study, for the first time, we have identified the p55 γ regulatory subunit of PI3K as a target molecule of ALK during mouse fibroblast cell migration (Supplementary Fig. 9a). Physical

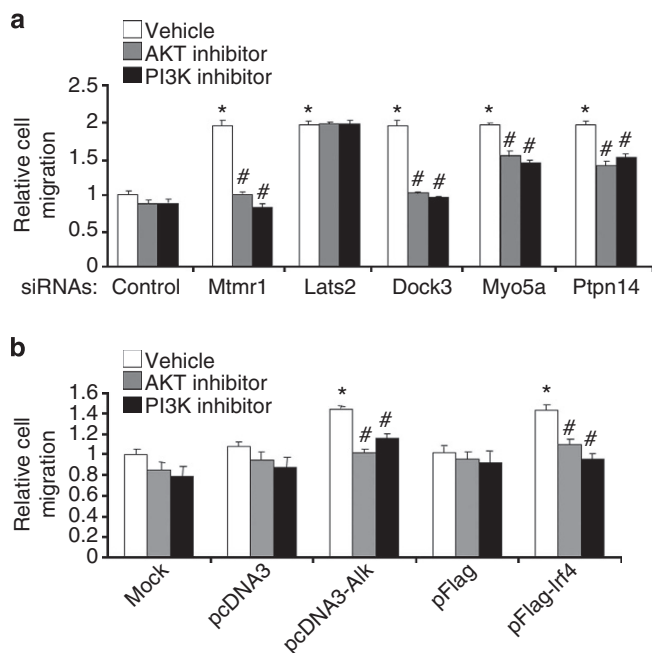


Figure 6 | Dependences of selected cell migration regulators on the PI3K/AKT pathway. (a) NIH3T3 cells were transiently transfected with control siRNA or siRNAs targeting *mtmr1* (#5), *lats2* (#3), *dock3* (#1), *myo5a* (#3) or *ptpn14* (#5). After 24 h, wound-healing assay was conducted and cell migration was quantified in the presence or absence of AKT inhibitor (5 μ M) or PI3K inhibitor (LY294002; 15 μ M). The results shown are means \pm s.d. ($n = 3$). * P -values of < 0.05 indicate significantly different from control siRNA-transfected cells; # P -values of < 0.05 indicate significantly different from the corresponding siRNA-transfected cells not treated with inhibitor. (b) Alternatively, NIH3T3 cells were transiently transfected with empty vector (*pcDNA3*) or *alk* or *irf4* expression constructs (*pcDNA3-alk* or *pFlag-irf4*) for 24 h. Wound-healing assay was performed to evaluate cell migration in the presence or absence of AKT inhibitor (5 μ M) or PI3K inhibitor (LY294002; 15 μ M). The results shown are mean \pm s.d. ($n = 3$). * P -values of < 0.05 indicate significantly different from *pcDNA3* or *pFlag* empty vector transfected cells; # P -values of < 0.05 indicate significantly different from the cells under a similar condition without the inhibitor treatment.

interaction between ALK and p55 γ , ALK-induced phosphorylation of p55 γ , and p55 γ knockdown studies supported these findings. NIH3T3 cells express three isoforms of AKT. When the involvement of AKT isoforms in the ALK-induced cell migration was examined by knockdown of individual isoforms of *akt* (*akt1*, *akt2* and *akt3*), all three isoforms of AKT were found to play an important role in the ALK-induced migration (Supplementary Fig. 10). Although the critical role of p55 γ in the ALK/AKT-induced cell migration has been demonstrated in the current study, it does not necessarily indicate that all the migration-related signalling is mediated via ALK/AKT and p55 γ . Also, the phosphorylation of the regulatory subunit p55 γ should not be regarded as a definitive indication for increased migration, as the cell migration depends on the relevant downstream PI3K targets and additional regulators. Further studies need to be conducted to better assess the importance of p55 γ in cell migration in general.

In summary, the selection method used in the present study allowed us to identify a large number of genes that modulated cell migration. Furthermore, many of the cell migration-regulating genes identified have not been previously associated with cell migration. Although the precise regulatory mechanisms responsible for the effects of these cell migration regulators will only be

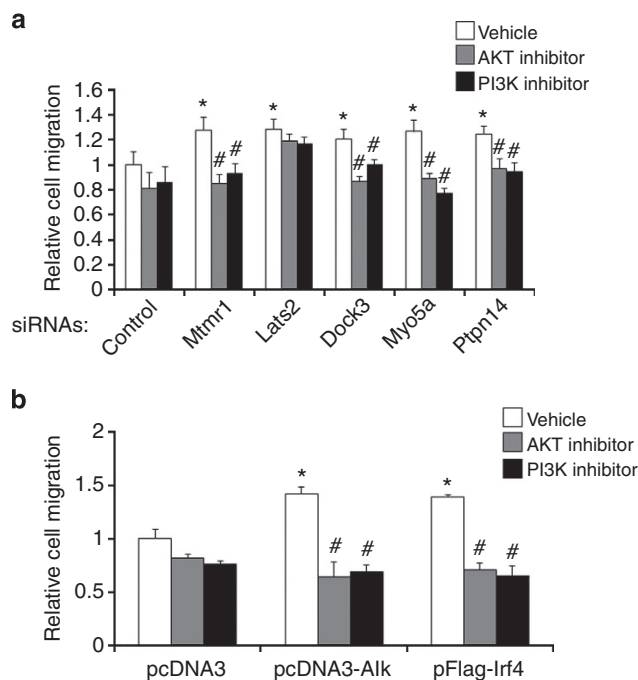


Figure 7 | Dependence of selected cell migration regulators on the PI3K/AKT pathway determined by three-dimensional cell migration assay.

NIH3T3 cells were transiently transfected with either siRNAs targeted for *mtmr1*, *lats2*, *dock3*, *myo5a* and *ptpn14* (a) or *alk* and *irf4* expression constructs (*pcDNA3-alk* or *pFlag-irf4*) (b). After 24 h of transfection, NIH3T3 fibroblast cells (4×10^4 cells/well) were seeded onto the transwell culture inserts and incubated in the presence or absence of either AKT inhibitor (5 μ M) or PI3K inhibitor (LY294002; 15 μ M) at 37 $^{\circ}$ C for 6 h. After incubation, non-migrated cells were removed from the upper face of the transwell culture insert. The cells that migrated across the membrane were stained and counted as described in the main text. The results are mean \pm s.d. ($n = 3$). * $P < 0.05$ represents significantly different from control siRNA-transfected cells; # $P < 0.05$ represents significantly different from the corresponding siRNA-transfected cells without the inhibitor treatment.

determined by additional studies, the candidate gene list obtained by the current selection process provides an integrated view regarding cell migration.

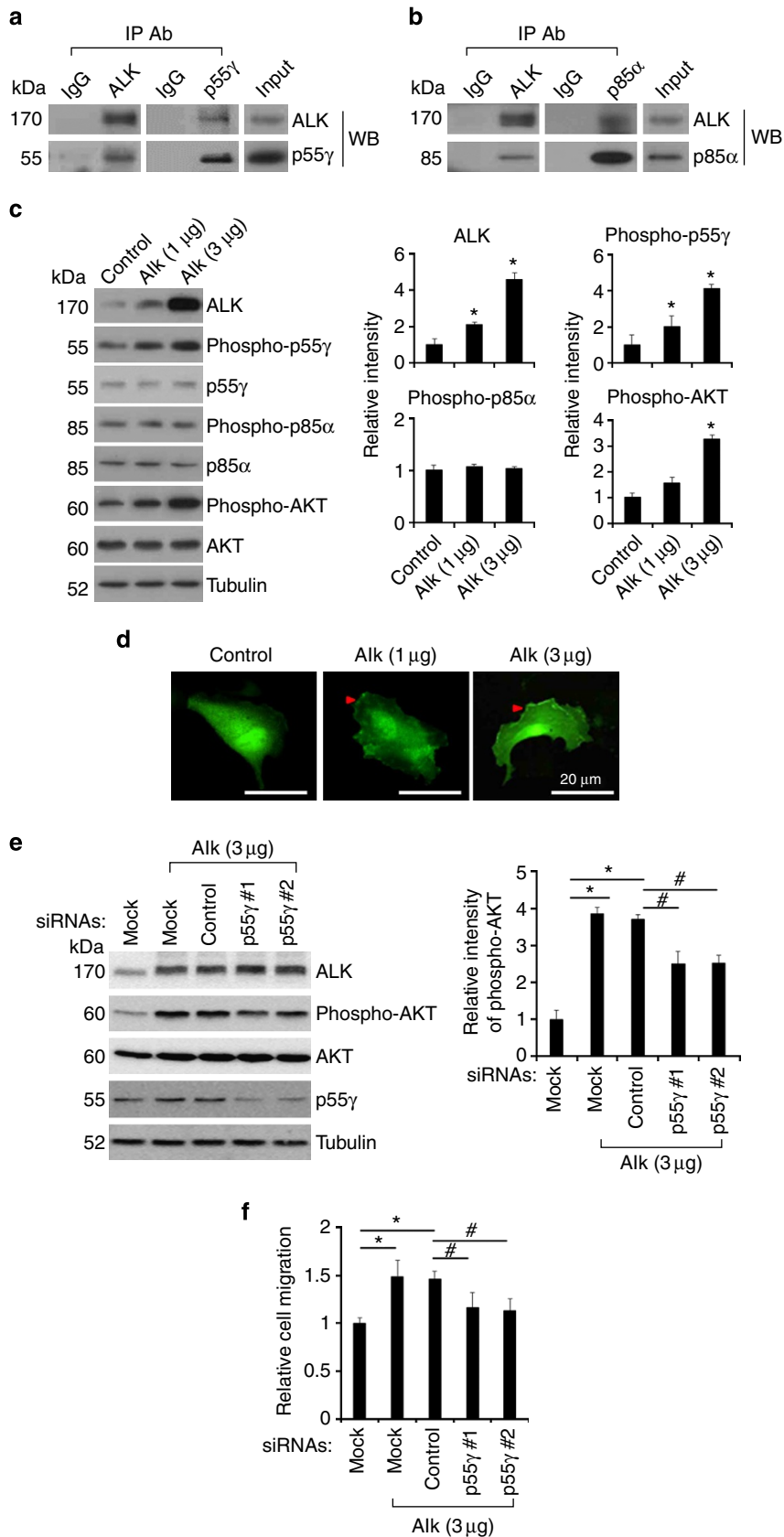
Methods

Reagents and cells. Specific small-molecule inhibitors, such as Akt inhibitor (1L6-hydroxymethyl-chiro-inositol-2-(R)-2-O-methyl-3-O-octadecyl-*sn*-glycerocarboxon) and PI3K inhibitor (LY294002), were purchased from Calbiochem (La Jolla, CA). Puromycin and mitomycin C were purchased from Sigma-Aldrich (St Louis, MO). All other chemicals, unless otherwise stated, were obtained from Sigma-Aldrich. NIH3T3 mouse fibroblast cells, L929 mouse fibroblast cells and HEK293T human embryonic kidney epithelial cells were maintained in Dulbecco's modified Eagle's media (DMEM) supplemented with 10% heat-inactivated fetal bovine serum (FBS) (Invitrogen, Carlsbad, CA), 100 U ml $^{-1}$ penicillin and 100 μ g ml $^{-1}$ streptomycin (Gibco-BRL, Rockville, MD). Phoenix Ampho cells were cultured in DMEM containing 10% FBS (Lonza, Walkersville, MD), hygromycin B (300 μ g ml $^{-1}$) and diphtheria toxin (1 μ g ml $^{-1}$) at 37 $^{\circ}$ C and 5% CO $_2$. MEF cell cultures were prepared from 13.5-day-old embryos of Institute for Cancer Research (ICR) mice⁶⁸.

Lentivirus production and titration. A 63,996 pooled lentiviral shRNA library targeting 21,332 mouse genes was generated by the transient transfection of HEK293T cells with *pHAGE-mir30-RFP-shRNA* (targeting the mouse genome), *pVSV-G*, *pTat*, *pPM2* and *pRev* using LipofectAMINE 2000 (Invitrogen), in accordance with the manufacturer's instructions. The mir30-based shRNA constructs have been previously described¹⁴. Cell-free supernatants were collected 2–3 days after transfection and were subsequently used to transduce NIH3T3 cells in the presence of 8 μ g ml $^{-1}$ polybrene. After 24 h, virus-containing supernatants

were removed by centrifugation. To optimize conditions for viral infection and to monitor virus titres, NIH3T3 fibroblast cells (1×10^6 cells) were seeded onto 100-mm culture plates 18 h before infection and then incubated with 1 ml of red fluorescence protein-carrying lentiviral stock for 6–8 h, in the presence of

polybrene ($8 \mu\text{g ml}^{-1}$). Fresh DMEM/10% FBS (2 ml) containing polybrene ($8 \mu\text{g ml}^{-1}$) was then added to the culture and incubation was continued. After another 24 h, cells were removed from plates, and infection efficiencies and viral titres were determined by observing red fluorescence protein under a fluorescence



microscope (Olympus BX50; Tokyo). The titre of the viral shRNA library was $\sim 7.23 \times 10^6$ p.f.u. ml⁻¹.

Selection of cell migration regulators using shRNA library. NIH3T3 fibroblast cells were seeded at the density of 1×10^6 cells/100-mm culture plate. Three plates of NIH3T3 cells were infected with the lentiviral shRNA library at an m.o.i. of 1 in the presence of polybrene ($8 \mu\text{g ml}^{-1}$) ($45 \times$ representation for each shRNA). Two days after infection, cells were puromycin (10 ng ml^{-1})-selected for 7 days, detached, seeded onto transwell culture inserts ($8\text{-}\mu\text{m}$ pore membrane; Millipore, Billerica, MA) in 24-well plates ($\sim 4 \times 10^4$ cells/transwell culture insert/well) and incubated at 37°C for either 5 or 24 h. The 5-h time point was used to select migration enhancers and 24 h was used to identify inhibitors of migration. Upper and lower transwell chambers were filled with media containing 0% or 10% FBS, respectively, to induce the directional movement of cells. Infected cells ($\sim 3 \times 10^6$ cells) were divided and placed onto 72 transwell culture inserts. Cells that did or did not migrate were collected by trypsinizing cells adherent to the lower or upper faces of transwell culture inserts, respectively, and then reseeded onto transwell culture inserts. Cells from 72 individual wells were then allowed to re-migrate five times for enrichment purposes. Selected cells from the 72 transwell culture inserts were then combined. To identify the shRNAs integrated into the combined cells, a small amount (50 ng) of genomic DNA separately isolated from migrating or non-migrating cells was subjected to PCR. shRNA segments were amplified using the primer set: forward primer *JH353F*, TAGTGAAGCCACAGATGTA; reverse primer *BC1R*, CCTCCCCTACCCGGTAGA¹⁴. The resulting PCR fragments (453 bp) were gel-purified, cloned and sequenced⁶⁹ (Fig. 1). All clones were sequenced. The sequences of 22–27 nt, corresponding to the half-hairpins of shRNAs, were used to identify shRNAs.

Validation of primary hits using retroviral shRNAs. Retroviral shRNAs were generated by transient transfection of Phoenix Amphi packaging cells with each shRNA using Lipofectamine 2000 in accordance with the manufacturer's instructions. Cell-free supernatants were harvested 2–3 days after transfection and subsequently were used to transduce NIH3T3 fibroblast cells in the presence of $8 \mu\text{g ml}^{-1}$ polybrene. To optimize conditions of viral infection and to monitor viral titre, a test construct of the retroviral vector carrying GFP (*pFB-hrGFP*) (Stratagene) was used. For infection of NIH3T3 fibroblast cells, cells (1×10^5 cells/well) were seeded onto 60-mm culture plates 18 h before infection and incubated with 1 ml of virus stock for 6–8 h in the presence of polybrene ($8 \mu\text{g ml}^{-1}$). Then, 2 ml of fresh DMEM/10% FBS containing polybrene ($8 \mu\text{g ml}^{-1}$) was added to the culture and the incubation was continued. After another 24 h, cells were removed from the plates, and infection efficiency and viral titre were determined by the count of GFP-positive cells using FACS. NIH3T3 fibroblast cells were infected with the retroviral shRNA at an m.o.i. of 1–3. For high-throughput screening, Essen Incucyte and Woundmaker (Essen BioScience, Ann Arbor, MI) were used. In brief, the cell migration algorithm analyzed each image and assigned a well-specific wound mask that corresponded to the initial scratch wound. Scratch wound mask followed migrating cells as they moved into the initial wound, creating a measurement of relative wound density or wound closure.

Pathway and network analyses. The accession numbers of identified DNAs were exported to IPA (Ingenuity Systems) for network analysis. The statistical significance of each network or list was determined by IPA using Fisher's Exact test ($P < 0.05$). IPA was also used to construct networks of protein–protein and other regulatory interactions. For pathway construction, the IPA database used currently available knowledge on genes, proteins, chemicals, normal and disease cellular processes, signalling and cellular functions.

Transient transfection with siRNA or cDNA. Desalted and preannealed siRNA duplexes were purchased from Genolution Pharmaceuticals (Seoul, Korea). The

siRNAs were designed using a proprietary algorithm devised by Genolution Pharmaceuticals. Sequence information for the siRNAs used for validation is given in Supplementary Table 6. To knockdown specific gene expression, NIH3T3 mouse fibroblast cells were transfected with siRNAs at a final concentration of 10 nM using LipofectAMINE (Invitrogen), according to the manufacturer's instructions. Cells were harvested 24–48 h after transfection, and the potencies of siRNAs to silence gene expression were measured by RT-PCR or western blot analysis. A control random sequence siRNA was also purchased from Genolution Pharmaceuticals and used as negative control. The full-length cDNAs of mouse *alk* or *irf4* were cloned into the expression vectors *pcDNA3* or *pFlag*, respectively. NIH3T3 fibroblast cells in six-well plates were transiently transfected with $3 \mu\text{g}$ of *alk* or *irf4* cDNA using LipofectAMINE. The empty vector *pcDNA3* or *pFlag* was used as control for the transient expression of *alk* or *irf4*. One or two days after transfection, cells were used for experiments. The expressions of *alk* and *irf4* mRNAs and proteins in transient transfectants were confirmed by RT-PCR or western blot analysis, respectively.

Reverse transcription-PCR. Total RNA was extracted from NIH3T3 cells in six-well plates using TRIzol reagent (Invitrogen), according to the manufacturer's instructions. Reverse transcription was conducted using Superscript II (Invitrogen) and oligo(dT) primer. PCR amplification, using specific primer sets, was carried out at an annealing temperature of $55\text{--}60^\circ\text{C}$ for 20–30 cycles. PCR was performed by using a DNA Engine Tetrad Peltier Thermal Cycler (MJ Research, Waltham, MA). To analyse PCR products, $10 \mu\text{l}$ of each PCR reaction product was electrophoresed on 1% agarose gel followed by ethidium bromide staining and detection under UV light. β -Actin was used as internal control. The nucleotide sequences of the primers used were based on published cDNA sequences (Supplementary Table 8).

Wound-healing assay. For the *in vitro* wound-healing assay, a scratch was created by using a $10\text{-}\mu\text{l}$ pipette tip on confluent cell monolayers in 24-well culture plates, and then DMEM containing 10% FBS, 100 U ml^{-1} penicillin and $100 \mu\text{g ml}^{-1}$ streptomycin was added. Cells were then incubated at 37°C under 5% CO_2 to enable migration into wounds, which were then observed under a light microscope (Olympus CK2; X100). To rule out confounding effect of cell proliferation, cells were treated with the mitosis inhibitor mitomycin-C at a final concentration of $10 \mu\text{g ml}^{-1}$ for 2 h before wounding. Relative cell migration distances were calculated by subtracting final wound widths from initial values⁷⁰. Three non-overlapping fields were selected and examined per well (three wells per experimental group). The results are presented as fold increases in migration distance versus control condition.

Three-dimensional cell migration assay. Cell migration was also measured using transwell culture inserts ($8\text{-}\mu\text{m}$ pore membrane; Millipore), according to the manufacturer's instructions. In brief, cells were transfected with the siRNAs of migration accelerating or impairing genes. At 24 h after transfection, cells were harvested by trypsinization, resuspended in DMEM and added to upper wells at 4×10^4 cells/well. Growth media were placed into base wells, which were separated from top wells by a polycarbonate filter membrane. Cells were incubated at 37°C for 6 h (for accelerating siRNAs) or 9 h (for impairing siRNAs). Non-migrating cells on the inner sides of transwell culture inserts were then removed with a cotton swab, and migrated cells on the undersides of inserts were fixed with methanol for 10 min and stained with Mayer's haematoxylin (DakoCytomation, Glostrup, Denmark) for 20 min. Photomicrographs of five random fields were taken (Olympus CK2; X100), and cells were then counted using a NIH image J program (NIH Image; Bethesda, MD). In brief, images were binary thresholded at 50% of the background level, and particles were then converted to a sub-threshold image area with a size > 200 pixels, which was determined to be sufficient to identify migrated cells. Numbers of cells were counted and results were analysed statistically.

Figure 8 | Pivotal role of p55 γ subunit of PI3K in Alk-mediated cell migration. (a, b) NIH3T3 fibroblast cells were used to reciprocally immunoprecipitate (IP) with anti-ALK and anti-PI3K antibodies as indicated. The precipitated protein was separated on SDS-PAGE and subjected to reciprocal western blot analysis (WB) using each antibody. (c) NIH3T3 fibroblast cells were transiently transfected with control vector (*pcDNA3*) or *alk* expression constructs (*pcDNA3-alk*). After 48 h, levels of phosphorylated or total ALK, p55 γ , p85 α and AKT were evaluated by western blotting. Tubulin was used as a loading control. The results of densitometric analysis (*right*) are mean \pm s.d. ($n = 3$); * P -values of < 0.05 indicate significantly different from control vector-transfected cells. (d) NIH3T3 fibroblast cells on coverslips were transiently transfected with GFP-*akt*-PH expression construct and control vector (*pcDNA3*) or *alk* expression constructs (*pcDNA3-alk*). After 36 h, transfected NIH3T3 fibroblast cell images were obtained using fluorescence microscopy to determine the localization of the GFP-AKT-PH. Arrowheads indicate plasma membrane-localized GFP-AKT-PH. Scale bar, $20 \mu\text{m}$. (e) ALK-overexpressing NIH3T3 fibroblast cells were transiently transfected with control siRNA or siRNAs against p55 γ . After 48 h, levels of total or phosphorylated AKT, ALK and p55 γ were evaluated by western blotting. Tubulin was used as a loading control. The results of phospho-AKT densitometry (*right*) are means \pm s.d. ($n = 3$). (f) After 24 h of transfection, NIH3T3 fibroblast cells (4×10^4 cells/well) were seeded onto the transwell culture inserts and incubated at 37°C for 9 h. The cells that migrated across the membrane were stained and counted as described in the main text. The results shown are means \pm s.d. ($n = 3$); * P -values of < 0.05 indicate significantly different from empty vector-transfected cells. # P -values of < 0.05 indicate significantly different from control siRNA-transfected cells.

Western blot analysis. Cells were lysed in triple-detergent lysis buffer (50 mM Tris-HCl, pH 8.0, 150 mM NaCl, 0.02% sodium azide, 0.1% SDS, 1% NP-40, 0.5% sodium deoxycholate and 1 mM phenylmethylsulfonyl fluoride). Protein concentrations in cell lysates were determined using the Bio-Rad protein assay kit (Bio-Rad, Hercules, CA). Equal amounts of protein were separated by 8 or 12% SDS-PAGE and transferred to Hybond ECL nitrocellulose membranes (Amersham Biosciences, Piscataway, NJ). Membranes were blocked with 5% skim milk and sequentially incubated with primary antibodies (rabbit polyclonal anti-phospho-PI3 kinase p85 α (Tyr458)/p55 γ (Tyr199) antibody (1:500 dilution; Cell Signaling Technology, Danvers, MA); rabbit polyclonal anti-PI3 kinase p85 α antibody (1:1,000 dilution; Cell Signaling Technology); goat polyclonal anti-p55 γ antibody (1:500 dilution; Santa Cruz, Santa Cruz, CA); rabbit polyclonal anti-phospho-AKT (Ser473) antibody (1:1,000 dilution; Cell Signaling Technology); rabbit polyclonal anti-AKT antibody (1:1,000 dilution; Cell Signaling Technology); rabbit polyclonal anti-phospho-FOXO1 (Ser256) antibody (1:500 dilution; Cell Signaling Technology); rabbit polyclonal anti-FOXO1 antibody (1:500 dilution; Cell Signaling Technology); rabbit polyclonal anti-phospho-p70S6 kinase (Thr389) antibody (1:1,000 dilution; Cell Signaling Technology); rabbit polyclonal anti-p70S6 kinase antibody (1:1,000 dilution; Cell signaling Technology); monoclonal anti- α -tubulin antibody (1:2,000 dilution; Sigma-Aldrich); rabbit polyclonal anti-MTMR1 antibody (1:500 dilution; Sigma-Aldrich); goat polyclonal anti-PTPN14 antibody (1:500 dilution; Santa Cruz); rabbit polyclonal anti-DOCK3 antibody (1:500 dilution; Abcam, Cambridge, MA); rabbit polyclonal anti-IRF4 antibody (1:500 dilution; Cell Signaling Technology); rabbit polyclonal anti-ALK antibody (1:500 dilution; Novus Biologicals, and HRP-conjugated secondary antibodies (1:10,000 dilution; anti-rabbit-, anti-mouse-, or anti-goat-IgG antibody; Amersham Biosciences), and then detected using an ECL detection kit (Amersham Biosciences).

Assessment of cell proliferation and viability by MTT assay. NIH3T3 cells in 96-well culture plates were transfected with siRNAs or cDNA constructs and incubated for 24–72 h. At each designated time point after transfection, culture media were removed, MTT (3-[4,5-dimethylthiazol-2-yl]-2,5-diphenyltetrazolium bromide) (0.5 mg ml⁻¹) was added and cells were incubated at 37 °C for 2 h in a CO₂ incubator. After dissolving the insoluble crystals that formed in DMSO, absorbance was measured at 570 nm using a microplate reader (Anthos Labtec Instruments, Wals, Austria).

Statistical analysis. Results are presented as the means \pm s.d. of three or more independent experiments, unless stated otherwise. The one-way ANOVA with Dunnett's multiple-comparison test was used to compare treatments. SPSS version 18.0 K (SPSS, Chicago, IL) was used for the analysis, and *P*-value differences of <0.05 were considered statistically significant.

References

- Vicente-Manzanares, M., Webb, D. J. & Horwitz, A. R. Cell migration at a glance. *J. Cell. Sci.* **118**, 4917–4919 (2005).
- Franz, C. M., Jones, G. E. & Ridley, A. J. Cell migration in development and disease. *Dev. Cell* **2**, 153–158 (2002).
- Luster, A. D., Alon, R. & von Andrian, U. H. Immune cell migration in inflammation: present and future therapeutic targets. *Nat. Immunol.* **6**, 1182–1190 (2005).
- Cram, E. J., Shang, H. & Schwarzbauer, J. E. A systematic RNA interference screen reveals a cell migration gene network in *C. elegans*. *J. Cell Sci.* **119**, 4811–4818 (2006).
- Wang, X. *et al.* Analysis of cell migration using whole-genome expression profiling of migratory cells in the *Drosophila* ovary. *Dev. Cell* **10**, 483–495 (2006).
- Dykxhoorn, D. M., Novina, C. D. & Sharp, P. A. Killing the messenger: short RNAs that silence gene expression. *Nat. Rev. Mol. Cell Biol.* **4**, 457–467 (2003).
- Paddison, P. J. *et al.* A resource for large-scale RNA-interference-based screens in mammals. *Nature* **428**, 427–431 (2004).
- Simpson, K. J. *et al.* Identification of genes that regulate epithelial cell migration using an siRNA screening approach. *Nat. Cell Biol.* **10**, 1027–1038 (2008).
- Vitorino, P. & Meyer, T. Modular control of endothelial sheet migration. *Gene Dev.* **22**, 3268–3281 (2008).
- Winograd-Katz, S. E., Itzkovitz, S., Kam, Z. & Geiger, B. Multiparametric analysis of focal adhesion formation by RNAi-mediated gene knockdown. *J. Cell Biol.* **186**, 423–436 (2009).
- Collins, C. S. *et al.* A small interfering RNA screen for modulators of tumor cell motility identifies MAP4K4 as a promigratory kinase. *Proc. Natl Acad. Sci. USA* **103**, 3775–3780 (2006).
- Bai, S. W. *et al.* Identification and characterization of a set of conserved and new regulators of cytoskeletal organization, cell morphology and migration. *BMC Biol.* **9**, 54–71 (2011).
- Smolen, G. A. *et al.* A genome-wide RNAi screen identifies multiple RSK-dependent regulators of cell migration. *Gene Dev.* **24**, 2654–2665 (2010).
- Schlabach, M. R. *et al.* Cancer proliferation gene discovery through functional genomics. *Science* **319**, 620–624 (2008).
- Silva, J. M. *et al.* Second-generation shRNA libraries covering the mouse and human genomes. *Nat. Genet.* **37**, 1281–1288 (2005).
- Yang, J. *et al.* Genome-wide RNAi screening identifies genes inhibiting the migration of glioblastoma cells. *PLoS ONE* **8**, e61915 (2013).
- Qian, Y. *et al.* PI3K induced actin filament remodeling through Akt and p70S6K1: implication of essential role in cell migration. *Am. J. Physiol. Cell Physiol.* **286**, C153–C163 (2004).
- Song, M. S., Salmena, L. & Pandolfi, P. P. The functions and regulation of the PTEN tumour suppressor. *Nat. Rev. Mol. Cell Biol.* **13**, 283–296 (2012).
- Martelli, A. M. *et al.* Targeting the translational apparatus to improve leukemia therapy: roles of the PI3K/PTEN/Akt/mTOR pathway. *Leukemia* **25**, 1064–1079 (2011).
- Schlessinger, J. & Ullrich, A. Growth factor signaling by receptor tyrosine kinases. *Neuron* **9**, 383–391 (1992).
- Raucher, D. *et al.* Phosphatidylinositol 4,5-bisphosphate functions as a second messenger that regulates cytoskeleton-plasma membrane adhesion. *Cell* **100**, 221–228 (2000).
- Zhu, Q. *et al.* Phosphoinositide 3-OH kinase p85 α and p110 β are essential for androgen receptor transactivation and tumor progression in prostate cancers. *Oncogene* **27**, 4569–4579 (2008).
- Kim, D. H. & Rossi, J. J. Strategies for silencing human disease using RNA interference. *Nat. Rev. Genet.* **8**, 173–184 (2007).
- Cheng, J. C., Moore, T. B. & Sakamoto, K. M. RNA interference and human disease. *Mol. Genet. Metab.* **80**, 121–128 (2003).
- Alvarez-Calderon, F., Gregory, M. A. & Degregori, J. Using functional genomics to overcome therapeutic resistance in hematological malignancies. *Immunol. Res.* **33**, 100–115 (2012).
- Dahlman, K. B. *et al.* Modulators of prostate cancer cell proliferation and viability identified by short-hairpin RNA library screening. *PLoS ONE* **7**, e34414 (2012).
- Hu, K., Law, J. H., Fotovati, A. & Dunn, S. E. Small interfering RNA library screen identified polo-like kinase-1 (PLK1) as a potential therapeutic target for breast cancer that uniquely eliminates tumor-initiating cells. *Breast Cancer Res.* **14**, R22 (2012).
- Wan, X. *et al.* Identification of the FoxM1/Bub1b signaling pathway as a required component for growth and survival of rhabdomyosarcoma. *Cancer Res.* **72**, 5889–5899 (2012).
- Draviam, V. M. *et al.* A functional genomic screen identifies a role for TAO1 kinase in spindle-checkpoint signalling. *Nat. Cell Biol.* **9**, 556–564 (2007).
- Root, D. E., Hacohen, N., Hahn, W. C., Lander, E. S. & Sabatini, D. M. Genome-scale loss-of-function screening with a lentiviral RNAi library. *Nat. Methods* **3**, 715–719 (2006).
- Hu, G. *et al.* A genome-wide RNAi screen identifies a new transcriptional module required for self-renewal. *Gene Dev.* **23**, 837–848 (2009).
- Schmitz, M. H. *et al.* Live-cell imaging RNAi screen identifies PP2A-B55 α and importin- β 1 as key mitotic exit regulators in human cells. *Nat. Cell Biol.* **12**, 886–893 (2010).
- Yang, R. *et al.* A genome-wide siRNA screen to identify modulators of insulin sensitivity and gluconeogenesis. *PLoS ONE* **7**, e36384 (2012).
- Romieu-Mourez, R., Landesman-Bollag, E., Seldin, D. C. & Sonenshein, G. E. Protein kinase CK2 promotes aberrant activation of nuclear factor- κ B, transformed phenotype, and survival of breast cancer cells. *Cancer Res.* **62**, 6770–6778 (2002).
- Channavajhala, P. & Seldin, D. C. Functional interaction of protein kinase CK2 and c-Myc in lymphomagenesis. *Oncogene* **21**, 5280–5288 (2002).
- Munstermann, U. *et al.* Casein kinase II is elevated in solid human tumours and rapidly proliferating non-neoplastic tissue. *Eur. J. Biochem.* **189**, 251–257 (1990).
- Zhang, P. *et al.* Identification and functional characterization of p130Cas as a substrate of protein tyrosine phosphatase nonreceptor 14. *Oncogene* **32**, 2087–2095 (2012).
- Buj-Bello, A. *et al.* Muscle-specific alternative splicing of myotubularin-related 1 gene is impaired in DM1 muscle cells. *Hum. Mol. Genet.* **11**, 2297–2307 (2002).
- Tronchere, H. *et al.* Production of phosphatidylinositol 5-phosphate by the phosphoinositide 3-phosphatase myotubularin in mammalian cells. *J. Biol. Chem.* **279**, 7304–7312 (2004).
- Ryeom, S. *et al.* Targeted deletion of the calcineurin inhibitor DSCR1 suppresses tumor growth. *Cancer Cell* **13**, 420–431 (2008).
- Aylon, Y. *et al.* A positive feedback loop between the p53 and Lats2 tumor suppressors prevents tetraploidization. *Genes Dev.* **20**, 2687–2700 (2006).
- McPherson, J. P. *et al.* Lats2/Kpm is required for embryonic development, proliferation control and genomic integrity. *EMBO J.* **23**, 3677–3688 (2004).
- Ke, H. *et al.* Putative tumor suppressor Lats2 induces apoptosis through downregulation of Bcl-2 and Bcl-x(L). *Exp. Cell Res.* **298**, 329–338 (2004).
- Li, Y. *et al.* Lats2, a putative tumor suppressor, inhibits G1/S transition. *Oncogene* **22**, 4398–4405 (2003).

45. Huang, H. & Tindall, D. J. Dynamic FoxO transcription factors. *J. Cell Sci.* **120**, 2479–2487 (2007).
46. Zhang, H. *et al.* FOXO1 inhibits Runx2 transcriptional activity and prostate cancer cell migration and invasion. *Cancer Res.* **71**, 3257–3267 (2011).
47. Huang, H. & Tindall, D. J. Regulation of FOXO protein stability via ubiquitination and proteasome degradation. *Biochim. Biophys. Acta* **1813**, 1961–1964 (2011).
48. Brunet, A. *et al.* Akt promotes cell survival by phosphorylating and inhibiting a Forkhead transcription factor. *Cell* **96**, 857–868 (1999).
49. Meng, Q., Xia, C., Fang, J., Rojanasakul, Y. & Jiang, B. H. Role of PI3K and AKT specific isoforms in ovarian cancer cell migration, invasion and proliferation through the p70S6K1 pathway. *Cell Signal.* **18**, 2262–2271 (2006).
50. Liu, L. *et al.* Rapamycin inhibits cell motility by suppression of mTOR-mediated S6K1 and 4E-BP1 pathways. *Oncogene* **25**, 7029–7040 (2006).
51. Poon, M. *et al.* Rapamycin inhibits vascular smooth muscle cell migration. *J. Clin. Invest.* **98**, 2277–2283 (1996).
52. Bunney, T. D. & Katan, M. Phosphoinositide signalling in cancer: beyond PI3K and PTEN. *Nat. Rev. Cancer* **10**, 342–352 (2010).
53. Inukai, K. *et al.* Five isoforms of the phosphatidylinositol 3-kinase regulatory subunit exhibit different associations with receptor tyrosine kinases and their tyrosine phosphorylations. *FEBS Lett.* **490**, 32–38 (2001).
54. Vanhaesebroeck, B., Guillermet-Guibert, J., Graupera, M. & Bilanges, B. The emerging mechanisms of isoform-specific PI3K signalling. *Nat. Rev. Mol. Cell Biol.* **11**, 329–341 (2010).
55. Courtney, K. D., Corcoran, R. B. & Engelman, J. A. The PI3K pathway as drug target in human cancer. *J. Clin. Oncol.* **28**, 1075–1083 (2010).
56. Hu, J. *et al.* Overexpression of the N-terminal end of the p55gamma regulatory subunit of phosphatidylinositol 3-kinase blocks cell cycle progression in gastric carcinoma cells. *Int. J. Oncol.* **26**, 1321–1327 (2005).
57. Wang, G. *et al.* PI3K stimulates DNA synthesis and cell-cycle progression via its p55PIK regulatory subunit interaction with PCNA. *Mol. Cancer Ther.* **12**, 2100–2109 (2013).
58. Wang, G. *et al.* Blocking p55PIK signaling inhibits proliferation and induces differentiation of leukemia cells. *Cell Death Differ.* **19**, 1870–1879 (2012).
59. Wang, G. *et al.* p55PIK-PI3K stimulates angiogenesis in colorectal cancer cell by activating NF-kappaB pathway. *Angiogenesis* **16**, 561–573 (2013).
60. Zhang, L. *et al.* Integrative genomic analysis of phosphatidylinositol 3'-kinase family identifies PIK3R3 as a potential therapeutic target in epithelial ovarian cancer. *Clin. Cancer Res.* **13**, 5314–5321 (2007).
61. Waite, K. & Eickholt, B. J. The neurodevelopmental implications of PI3K signaling. *Curr. Top. Microbiol. Immunol.* **346**, 245–265 (2010).
62. Roskoski, Jr. R. Anaplastic lymphoma kinase (ALK): structure, oncogenic activation, and pharmacological inhibition. *Pharmacol. Res.* **68**, 68–94 (2013).
63. Polgar, D. *et al.* Truncated ALK derived from chromosomal translocation t(2;5)(p23;q35) binds to the SH3 domain of p85-PI3K. *Mutat. Res.* **570**, 9–15 (2005).
64. Wasik, M. A. *et al.* Anaplastic lymphoma kinase (ALK)-induced malignancies: novel mechanisms of cell transformation and potential therapeutic approaches. *Semin. Oncol.* **36**, S27–S35 (2009).
65. Palmer, R. H., Vernersson, E., Grabbe, C. & Hallberg, B. Anaplastic lymphoma kinase: signalling in development and disease. *Biochem. J.* **420**, 345–361 (2009).
66. Iwahara, T. *et al.* Molecular characterization of ALK, a receptor tyrosine kinase expressed specifically in the nervous system. *Oncogene* **14**, 439–449 (1997).
67. Yao, S. *et al.* Anaplastic lymphoma kinase is required for neurogenesis in the developing central nervous system of zebrafish. *PLoS ONE* **8**, e63757 (2013).
68. Serrano, M., Lin, A. W., McCurrach, M. E., Beach, D. & Lowe, S. W. Oncogenic ras provokes premature cell senescence associated with accumulation of p53 and p16INK4a. *Cell* **88**, 593–602 (1997).
69. Seo, M., Lee, W. H. & Suk, K. Identification of novel cell migration-promoting genes by a functional genetic screen. *FASEB J.* **24**, 464–478 (2010).
70. Bassi, R. *et al.* HMGB1 as an autocrine stimulus in human T98G glioblastoma cells: role in cell growth and migration. *J. Neurooncol.* **87**, 23–33 (2008).

Acknowledgements

This work was supported by the National Research Foundation of Korea (NRF) grant funded by the Korea government (MSIP) (Nos 2008-0062282 and 2012M3A9B6055414) and by a grant from the Korean Health technology R&D Project, Ministry of Health & Welfare, Republic of Korea (A111345). This work was also supported by a DOD Breast Cancer Innovator Award and a grant from SU2C to S.J.E. at the Howard Hughes Medical Institute. The authors thank Dr Young-il Park at Young-il Sciences Inc. (Daegu, Korea) for generously providing Incucyte and Woundmaker (Essen BioScience, Ann Arbor, MI).

Author contributions

M.S. and S.L. performed the experiments, analysed the data and prepared the manuscript. J.-H.K. performed the biochemical assays. W.-H.L. analysed the data. G.H. and S.J.E. provided reagents and analysed the data. K.S. directed the study and were involved in all aspects of the experimental design, data analysis and manuscript preparation. All authors critically reviewed the text and figures.

Additional information

Supplementary Information accompanies this paper at <http://www.nature.com/naturecommunications>

Competing financial interests: The authors declare no competing financial interests.

Reprints and permission information is available online at <http://npg.nature.com/reprintsandpermissions/>

How to cite this article: Seo, M. *et al.* RNAi-based functional selection identifies novel cell migration determinants dependent on PI3K and AKT pathways. *Nat. Commun.* **5**:5217 doi: 10.1038/ncomms6217 (2014).